Deformations of the Weyl Character Formula for $SO(2n + 1)$ via Ice Models

Yulia Alexandr[*] Patricia Commins[†] Alexandra Embry[‡] Sylvia Frank[§]
Yutong Li[¶] Alexander Vetter[‖]

October 1, 2018

Abstract

The irreducible representations of complex Lie groups are often encoded by Young tableaux and then explored further using combinatorial techniques. Many interesting results have been obtained for Cartan types A and C from the tableaux that describe their branching rules. The main goal of this paper is to study different types of Young tableaux that stem from branching rules of $SO(2n + 1, \mathbb{C})$ representations. In particular, we study highest weight characters of $SO(2n + 1, \mathbb{C})$ using statistical mechanics. We explore properties of tetravalent graphs known as ice models, using the Yang-Baxter equation and similar relations. A special type of an ice model is introduced, where the top row is a 5-vertex model, that is in bijection with the tableaux rules described by Sundaram. We show these ice models are in bijection with a variant of Gelfand-Tsetlin patterns, which are in turn in bijection with certain shifted Young tableaux. We then define a partition function over the admissible states of an ice model, which is shown to correspond to a deformation of the Weyl character formula for Cartan type B. We also introduce an ice model with every third row being a 3-vertex model for the tableaux rules described by Koike and Terada as well as show that there exist no ice model in bijection with tableaux described by Proctor.

1 Introduction

The mathematical framework of statistical mechanics is closely related to the theory of group representations. In particular, it involves combinatorial manifestations of the Weyl character formula. We wish to study deformations of this formula and its relationship with a type of tetravalent graphs called ice models, which can find applications in the description of many combinatorial and representation theoretical problems. Kuperberg[10] used these models to solve the problem of counting classes of alternating sign matrices. In [2], using ice models, the authors recovered deformations due to Okada [12].

[*]Wesleyan University, CT
[†]Carleton College, MN
[‡]Indiana University, IN
[§]Amherst College, MA
[¶]Haverford College, PA
[‖]Villanova University, PA

The study of representations using combinatorial objects began with Tokuyama[15], who gave a deformation of the Weyl character formula in the case of $GL(n, \mathbb{C})$ through the use of strict Gelfand-Tsetlin patterns. Brubaker et al. [1] supplied an alternative proof of Tokuyama's formula using the Yang-Baxter Equation. It turns out to be of big interest, since ice models, also known as solvable lattice models, are the starting point for the study of objects of further mathematical interests to many, like quantum groups and knot invariants. Further, the weight of particular ice models corresponds to Fourier coefficients of analytic L-functions.

The process of translating a group's representations into ice models involves several steps. First, given some tableaux rules (which stem from branching rules of a group's representations), we aim to display a bijection between the tableaux following those rules and some Gelfand-Tsetlin-type patterns. Then, we restrict our attention to only strict Gelfand-Tsetlin-type patterns and the corresponding shifted tableaux – purely combinatorial objects that are in correspondence with them. Next, we construct an ice state in bijection with each Gelfand-Tsetlin-type pattern, and thus with some shifted tableau. Finally, we assign Boltzmann weights to the vertices in the resulting ice model such that the partition function, summing over all admissible states, is equal to the product of the type B deformation and the Weyl character formula for $SO(2n+1, \mathbb{C})$. Following these steps, we obtain a fully functioning model for the tableaux first introduced by Sundaram, partial results for the tableaux described by Koike and Terada, and show that no ice model can properly describe the branching rules that Proctor's orthogonal tableaux encode.

2 Preliminaries

To help the reader become familiar with our study of the deformed characters of $SO(2n+1, \mathbb{C})$, we introduce the topic using the well-studied case of $GL(n, \mathbb{C})$. We first introduce the Weyl character formula. In order to study the deformations of this formula, we turn to the following combinatorial objects: Gelfand-Tsetlin patterns, strict Gelfand-Tsetlin patterns, semistandard Young tableaux, shifted Young tableaux, and ice models.

2.1 Weyl Character Formula

Let π be an irreducible, finite-dimensional representation of a complex semisimple Lie algebra $\mathfrak{g}$. Let $\mathfrak{h}$ be a Cartan subalgebra of $\mathfrak{g}$. Then, we can define the character of the irreducible representation $ch_\pi(H) : \mathfrak{h} \to \mathbb{C}$ by

$$ch_\pi(H) = tr(e^{\pi(H)}) \tag{1}$$

This character can be determined based upon the highest weight of π. We can define any highest weight λ and obtain the character of an irreducible representation through the Weyl character formula. The Weyl character formula is equivalent to:

Proposition 2.1.1 (Weyl Character Formula)**.**

$$ch_\pi(H) = \frac{\sum_{w \in W} (-1)^{l(w)} e^{w(\lambda+\rho)(H)}}{\sum_{w \in W} (-1)^{l(w)} e^{w(\rho)(H)}},$$

where W is a Weyl group, ρ is the half sum of the positive roots of the corresponding root system, λ is the highest weight of the irreducible representation, and $l(w)$ is the minimal length of the Weyl group element.

Corollary 2.1.1 (Weyl Character Formula for $GL(n,\mathbb{C})$)**.** *Let $\lambda = (\lambda_n \geq \lambda_{n-1} \geq \dots \lambda_1 \geq 0)$ index an irreducible representation of $GL(n,\mathbb{C})$ and let $s_\lambda(\mathbf{z})$ be the corresponding character, where $\mathbf{z} = (z_1, \dots, z_n)$. Let $\rho = (n-1, n-2, \dots, 0)$. Then, the Weyl character formula says:*

$$s_\lambda(\mathbf{z}) = \frac{\sum_{w \in S_n} sgn(w) \mathbf{z}^{w(\lambda+\rho)}}{\sum_{w \in S_n} sgn(w) \mathbf{z}^{w(\rho)}} \tag{2}$$

where $w(\mu)$ is the n-tuple from applying the permutation of w to μ.

It is important to note that the result is always a symmetric function, in particular, the Schur polynomial. It turns out, we have very nice combinatorial objects that give us the above function.

2.2 Schur Polynomials

The Schur polynomial is a class of symmetric functions that, in representation theory, represent the character values for highest-weight irreducible polynomial representations of $GL(n,\mathbb{C})$. If $\lambda = (\lambda_n \geq \lambda_{n-1} \geq \cdots \geq \lambda_1 \geq 0)$ indexes an irreducible representation of $GL(n,\mathbb{C})$, then the Schur polynomial $s_\lambda(x_1, ..., x_n)$ is defined in two equivalent ways:

1. As a quotient of two alternating sums over the symmetric group S_n (the Weyl Character Formula).
2. As a generating function on tableaux of shape λ (appears in tableaux section).

2.3 Gelfand-Tsetlin Patterns

A Gelfand-Tsetlin pattern is a triangular array of non-negative integers:

$$\begin{array}{ccccccccc} a_{1,1} & & a_{1,2} & & \cdots & & a_{1,n-1} & & a_{1,n} \\ & a_{2,1} & & a_{2,2} & \cdots & a_{2,n-1} & & a_{2,n} & \\ & & & & \cdots & & & & \\ & & & a_{n-1,1} & & a_{n-1,2} & & & \\ & & & & a_{n,1} & & & & \end{array} \tag{3}$$

subject to:

1. $a_{i,j-1} \geq a_{i,j} \geq a_{i,j+1} \geq 0$
2. $a_{i-1,j} \geq a_{i,j} \geq a_{i-1,j+1}$

In strict Gelfand-Tsetlin patterns, we drop the equality on both sides in the first condition, thus requiring rows to be strictly decreasing. Let $GT(\lambda)$ be the set of Gelfand-Tsetlin patterns with top row λ, and R_i be the sum of the i^{th} row in the GT pattern. Then, the Schur polynomial can be described equivalently:

$$s_\lambda(\mathbf{z}) = \sum_{P \in GT(\lambda)} \mathbf{z}^{wt(P)}, \tag{4}$$

where $\mathbf{z}^{wt(P)} := z_1^{p_1} z_2^{p_2} \dots z_n^{p_n}$, and $wt(P)$ is the n-tuple $(p_1, p_2, \dots, p_n)$, with $p_i = R_i - R_{i+1}$ for $i \in \{1, \dots, n-1\}, p_n = R_n$.
Therefore, we have a combinatorial interpretation for the character formula of $GL(n,\mathbb{C})$. To see a different combinatorial interpretation, we now turn to Young tableaux.

2.4 Semistandard Young Tableaux

Let $\lambda = (\lambda_n \geq \lambda_{n-1} \geq \cdots \geq \lambda_1 \geq 0)$ be a partition. We fill a Young diagram of shape λ using the alphabet $\{1 < 2 < \cdots < n\}$ such that:

1. Rows are weakly increasing.
2. Columns are strictly increasing.

2.4.1 Bijection between Gelfand-Tsetlin Patterns and Semistandard Young Tableaux

Let $SSYT(\lambda)$ be the set of semistandard Young tableaux with shape λ. Then, we have the following result:

Theorem 2.4.1.

$$s_\lambda(\mathbf{z}) = \sum_{T \in SSYT} \mathbf{z}^{wt(T)} \tag{5}$$

where $\mathbf{z}^{wt(T)} = \prod_{i=1}^{n} z_i^{c(i)}$, *and* $c(i)$ *is the number of* i*'s in a tableau* T.

Given the two different combinatorial objects that describe the character of an irreducible representation, we have a bijection

$$SSYT(\lambda) \xleftrightarrow{\text{1 to 1}} GT(\lambda) \tag{6}$$

To move between tableaux and Gelfand-Tsetlin patterns, we can label the rows of a Gelfand-Tsetlin from bottom to top with the letters of our alphabet for $GL(n, \mathbb{C})$. The bottom entry corresponds with the number of 1 entries in the first row of the tableaux. Each entry in the second row of the pattern corresponds to the number of entries in the first and second rows of the tableaux, respectively. We fill in the boxes of the tableaux with 2s until the tableaux boxes are filled corresponding to the length given by the pattern entries in that row. We continue until the tableaux is of shape λ.

Example 2.4.1.

1	1	1

$$\begin{array}{ccccc} 5 & & 3 & & 2 \\ & 3 & & 3 & \\ & & 3 & & \end{array}$$

1	1	1
2	2	2

$$\begin{array}{ccccc} 5 & & 3 & & 2 \\ & 3 & & 3 & \\ & & 3 & & \end{array}$$

1	1	1	3	3
2	2	2		
3	3			

$$\begin{array}{ccccc} 5 & & 3 & & 2 \\ & 3 & & 3 & \\ & & 3 & & \end{array}$$

With the bijection above, we state the the main result in type A case.

2.5 Tokuyama's Formula

Let λ be a partition. Let $\rho = (n-1, n-2, \ldots, 0)$. Let $SGT(\lambda+\rho)$ be the set of strict Gelfand-Tsetlin patterns with top row $(\lambda + \rho)$. Let $T \in SGT(\lambda + \rho)$. Consider the tuples (a, b, c) in T such that:

$$\begin{array}{ccc} a & & b \\ & c & \end{array} \tag{7}$$

Definition 2.5.1. A **special entry** of a strict Gelfand-Tsetlin pattern is an entry c such that $a > c > b$. We define $S(T)$ to be the number of special entries.

Definition 2.5.2. A **left-leaning entry** of a strict Gelfand-Tsetlin pattern is an entry c such that $a = c$. We define $L(T)$ to be the number of left-leaning entries.

Tokuyama [15] found a relationship between strict Gelfand-Tsetlin patterns and the Schur polynomials:

Theorem 2.5.1 (Tokuyama's Formula)**.**

$$\prod_{1 \le i < j \le n} (z_i + t z_j) s_\lambda(\mathbf{z}) = \sum_{T \in SGT(\lambda+\rho)} (1+t)^{S(T)} t^{L(T)} \mathbf{z}^{wt(T)} \tag{8}$$

This type of formula is known as a deformed character.

In particular, when $t = -1$, this is exactly equivalent to the Weyl character formula. When $t = 0$, Tokuyama's formula gives the original description of the character in terms of Gelfand-Tsetlin patterns.

We also note an important connection to analytic number theory. By setting $t = \frac{-1}{q}$ in Tokuyama's formula, the right hand side equals the spherical Whittaker function over a p-adic field with residue characteristic q. This is a cornerstone of the theory of automorphic L-functions, thus we are interested in this formula for more than its combinatorial properties.

2.6 Shifted Young Tableaux

Shifted tableaux are in bijective correspondence with strict Gelfand-Tsetlin patterns. Let $\rho = (n-1, n-2, \ldots, 0)$. We consider a shifted Young tableaux to be of shape $\lambda + \rho$ by attaching a standard tableaux of shape ρ to the left side of the standard tableaux of shape λ. The example below illustrates this process.

Example 2.6.1. Let $\lambda = (5, 3, 2, 1)$, then the standard tableaux looks like:

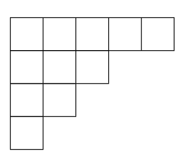

(9)

If we shift our tableaux by $\rho = (3, 2, 1, 0)$, then our new tableaux will look like:

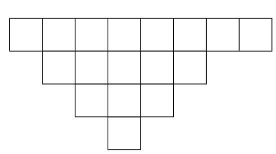

(10)

From this change, we have new rules for the filling the tableaux:

1. Rows are weakly increasing.
2. Columns are weakly increasing.
3. Diagonals are strictly increasing.

Let $SYT(\lambda+\rho)$ be the set of shifted Young tableaux that satisfy the above conditions. From these tableaux, we again have a bijection:

$$SYT(\lambda+\rho) \xleftrightarrow{\text{1 to 1}} SGT(\lambda+\rho) \tag{11}$$

We now move on to our main combinatorial object arising from statistical physics.

2.7 Ice Models

Definition 2.7.1. An ice state is a tetravalent directed graph.

In the case of $GL(n,\mathbb{C})$, we consider an ice state admissible if and only if there are two edges pointed to and from each vertex. Let $\lambda = (\lambda_n \geq \lambda_{n-1} \geq \cdots \geq \lambda_1 \geq 0)$ be a partition. We then obtain $(\lambda+\rho)$ and form an ice state subject to the following conditions:

1. There are n rows.
2. There are $\lambda_n + n$ columns, labeled from right to left $0, 1, 2, \ldots, \lambda_n + n - 1$.
3. We label the rows from bottom to top in increasing order of the alphabet for $GL(n,\mathbb{C})$.
4. All arrows on the left-hand side point to the right.
5. All arrows on the bottom point down.
6. All arrows on the right-hand side point to the left.
7. If $i \in (\lambda+\rho)$, the column i arrow points up; otherwise it points down.

The final four conditions are boundary conditions. We fill in the remaining edges such that every vertex has two arrows pointing in and two arrows pointing out. The admissible states of the ice models are in bijection with strict Gelfand-Tsetlin patterns. We can view the vertices of the ice model as points on a lattice. For $T \in SGT$, and $a_{i,j} \in T$, then the vertex in the i^{th} row from the top and in the column indexed by $a_{i,j}$ has an up arrow directly above it. The remaining column edges have down arrows. In particular, we have the bijection:

$$SGT(\lambda+\rho) \xleftrightarrow{\text{1 to 1}} ICE(\lambda+\rho) \tag{12}$$

2.7.1 Example of Ice Boundary Conditions

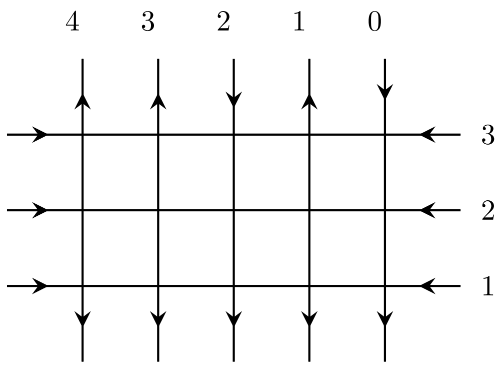

Figure 1: Ice Boundary Conditions for $\lambda + \rho = (4, 2, 1)$

2.7.2 Boltzmann Weights

Depending on the orientation of the arrows around a vertex, each vertex is assigned a particular Boltzmann weight. Invalid configurations of arrows have a Boltzmann weight of 0. The following are nonzero Boltzmann weights for the $GL(n, \mathbb{C})$ ice models as found in [1].

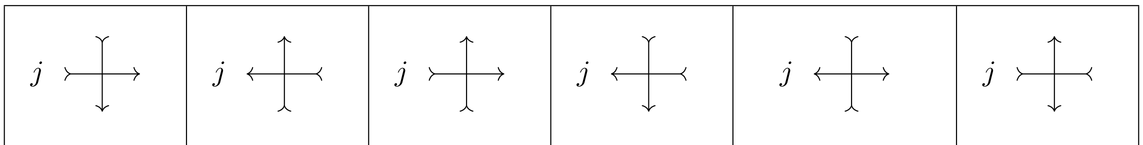

$NW = 1$	$SE = z_i$	$SW = t$	$NE = z_i$	$NS = z_i(t+1)$	$EW = 1$

Figure 2: Boltzmann weights for each of the six valid vertex orientations

2.7.3 Partition Function on Ice Models

From this description of ice models for $GL(n, \mathbb{C})$, we define a partition function $Z(\lambda)$. Let $ICE(\lambda+\rho)$ be the set of all admissible ice states with top row $\lambda+\rho$. For a particular $\mathcal{I} \in ICE(\lambda+\rho)$, assign the Boltzmann weights as in the previous section. Let $w(\mathcal{I})$ be the product of the Boltzmann weights of each vertex in the ice model. Then, our partition function is the following:

$$Z(\lambda) = \sum_{\mathcal{I} \in ICE} w(\mathcal{I}) \tag{13}$$

The following is proved in [1]:

Theorem 2.7.1.

$$Z(\lambda) = \prod_{1 \leq i < j \leq n} (z_i + t z_j) s_\lambda(\mathbf{z}) \tag{14}$$

Notice that the partition function is again an equivalent description of Tokuyama's formula, hence the deformed character of $GL(n, \mathbb{C})$.

2.8 Our Work

We follow the process in the previous section but consider the type B group $SO(2n+1,\mathbb{C})$. In particular, we look at three different types of tableaux due to Sundaram [14], Koike-Terada [9], and Proctor [13]. We create variants of Gelfand-Tsetlin patterns for each of these tableaux, and then show that strict GT patterns only exist for Sundaram and Koike-Terada tableaux. These strict patterns also give us a bijection to ice models with n boundary conditions. In the Sundaram case, we determine a set of Boltzmann weights that give us a deformation of the Weyl character formula for Cartan Type B. Further, we explore the origins of these tableaux through branching rules for $SO(2n+1,\mathbb{C})$.

We examine relationships between our combinatorial objects in the following way.

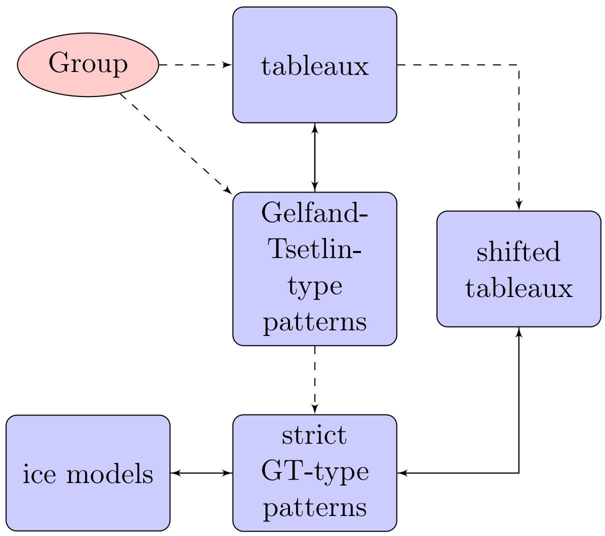

In this diagram, the black double-sided arrows represent bijections that are relatively easy to move between. The dotted arrows represent relationships that are less clear. Specifically, a group's representations' branching rules lead to a set of rules for tableaux and Gelfand-Tsetlin type patterns, but not all branching rules lead to tableaux and Gelfand-Tsetlin patterns that can eventually translate to ice models. Further, there are relationships between tableaux and shifted tableaux as well as between Gelfand-Tsetlin-type patterns and strict Gelfand-Tsetlin-type patterns. However, they are not in bijection, and the rules to move between them are less obvious and up to interpretation.

3 Sundaram Tableaux

3.1 Construction

Let $\lambda = (\lambda_n \geq \lambda_{n-1} \geq \dots \lambda_2 \geq 0)$ be a partition with n parts. Then, λ is the highest weight of an irreducible representation of $SO(2n+1)$. Further, we can find the character of this representation through the use of certain Young tableaux. Let λ define the length of the rows of such a tableaux. We fill the Young diagram with the alphabet $\{1 < \bar{1} < \cdots < n < \bar{n} < 0\}$ and the following rules:

1. Rows are weakly increasing.

2. Columns weakly increase, with strictly increasing nonzero entries.

3. No row contains multiple 0s.

4. In row i, all entries are greater than or equal to i.

We define the weight of a particular tableaux as the following:

$$\prod_{i=1}^{n} x^{w(i)-w(\bar{i})} \tag{15}$$

where $w(i)$ and $w(\bar{i})$ are the number of i and $\bar{i}$ in the Young tableaux. Sundaram shows that

$$s^{so}_{(\lambda)} = \sum_{T \in SSYT} \prod_{i=1}^{n} x^{w(i)-w(\bar{i})} \tag{16}$$

where SSYT is the set of Young diagrams filled according to the above rules, and $s^{so}_{(\lambda)}$ is the character of the irreducible representation of $SO(2n+1)$ indexed by λ.

3.2 Branching Rules

These tableaux rules derive from branching rules of the irreducible representations of $SO(2n+1, \mathbb{C})$, which we shall explore in the following section.

3.2.1 Relation to Sp(2n) Tableaux

Sundaram's tableaux for $SO(2n+1, \mathbb{C})$ is a result of the relationship:

$$s^{so}_{\lambda} = \sum_{\mu \subseteq \lambda} s^{sp}_{(\mu)} \tag{17}$$

where $\mu = (\mu_1 \geq \mu_2 \geq \ldots \mu_{n-1} \geq \mu_n > 0)$, s^{sp}_{μ} is the character of the irreducible representation of $Sp(2n)$ indexed by μ, and $\mu \subseteq \lambda$ if and only if $\lambda_i - \mu_i \leq 1$ for all i. Further, we can construct tableaux for $Sp(2n)$ using the exact same rules as the $SO(2n+1)$ tableaux, excluding 0 in the alphabet, as described by King [5]. Thus, it remains to understand the motivation for the tableaux rules for $Sp(2n)$.

3.2.2 Restriction of Sp(2n) Representations

In 1962, Zhelobenko showed the restriction $Sp(2n) \downarrow Sp(2n-2) \times U(1)$ is as follows [16]:

$$(\lambda) \downarrow = \sum_{x,y} (\lambda / x \cdot y)\{x - y\} \tag{18}$$

where x and y are one-partitions, and / and $\cdot$ are Schur function quotients and products determined by the Littlewood-Richardson rule, which is found in [8]. For our purposes λ/z means removing z boxes, no two from the same column. Further, x means the number of removals of n and y refers to the number of removals of $\bar{n}$. The tableaux construction from King arises because the formula above implies that the n^{th} row in T_λ has a value other than n or $\bar{n}$, then that tableaux vanishes in the restriction. Hence, the fourth condition in our tableaux rules is referred to as the symplectic condition on page 3160 in [8]. From that restriction relation, Wallach and Yacobi gave an explicit branching formula. Further, Howe, Lavicka, Lee, and Soucek describe this in terms of Young diagrams, and use it in order to produce a Skew Pieri rule for $Sp(2n)$ [6].

3.3 Gelfand-Tsetlin-Type Patterns

We define a new type of Gelfand-Tsetlin pattern that we will use to construct ice models. The patterns have the following shape:

$$\begin{array}{ccccccccccc}
a_{1,1} & & a_{1,2} & & \cdots & & & a_{1,n} & & & 0 \\
& a_{2,1} & & a_{2,2} & & \cdots & & & a_{2,n} & & \\
& & a_{3,1} & & a_{3,2} & & \cdots & & & a_{3,n} & \\
& & & & & \cdots & & & & & \\
& & & & & a_{2n-2,1} & & & a_{2n-2,2} & & \\
& & & & & & a_{2n-1,1} & & & a_{2n-1,2} & \\
& & & & & & & & a_{2n,1} & & \\
& & & & & & & & & a_{2n+1,1} &
\end{array} \tag{19}$$

and they following the same interleaving rules in Section 2.3.

3.4 Shifted Tableaux and Strict Gelfand-Tsetlin-Type Patterns

In this case, our shifted tableaux rules are the following:

1. Rows are weakly increasing.
2. Columns are weakly increasing.
3. Diagonals are strictly increasing.
4. No row contains consecutive 0s.
5. The first entry in row i is either i or $\bar{i}$.

For us, we only want strict Gelfand-Tsetlin-type patterns in order to construct valid corresponding ice models. In the Sundaram case, in order to biject with the shifted tableaux, our "strict" Gelfand-Tsetlin-type patterns will include the following constraints:

1. $a_{i,j-1} > a_{i,j} > a_{i,j+1} \geq 0$
2. $a_{2k,n-k+1} \neq 0$
3. $a_{1,k} - a_{2,k} \leq 1$

The first condition, which simply means that each row in our pattern is strictly increasing, allows us to create an ice model out of these patterns. The second condition is precisely equivalent to condition 5 of our shifted tableaux. The third condition is equivalent to the fourth condition of our shifted tableaux. Notice that the top row of our pattern is exactly equivalent to $\lambda + \rho$ and we add a 0 at the end for convenience.

Lemma 3.4.1. *For a given partition λ, we form the shifted tableaux of shape $\lambda + \rho$, and we let our top row of our Gelfand-Tsetlin pattern be equivalent to $\lambda + \rho$ with a 0 at the end. The permissible fillings of the shifted tableaux are in bijection with these Gelfand-Tsetlin type patterns.*

Proof. We propose an reversible algorithm for this process.
First, let row $2n+1$ of our Gelfand-Tsetlin type pattern correspond to filling the tableaux with 1, let row $2n$ correspond to filling with $\bar{1}$, and in general, let row $2k+1$ correspond to n-k+1 and let row $2k$ correspond to $\overline{n-k+1}$ for $k \geq 1$. Finally, let row 1 of the pattern correspond to filling with 0.
Beginning from the bottom row of the Gelfand-Tsetlin type pattern, we fill out the shifted tableaux using the numbers just described, as done in the General linear case. It is easy to see that Constraint 2 of the strict Gelfand-Tsetlin type patterns implies that either i or $\bar{i}$ will be on the main diagonal of row i in the tableaux. This algorithm also clearly forces our rows to be weakly increasing. Further, because the rows of the Gelfand-Tsetlin pattern are strictly decreasing, our corresponding columns will be weakly increasing. Further, condition 4 ensures that we do not add two 0s to any row in the shifted tableaux. Additionally, all diagonals are strictly increasing increasing because of our strict decreasing conditions in the GT model.
We claim that this algorithm is reversible. In particular, we can form a GT pattern from the bottom up by looking at the filled shifted tableaux. The conditions are clear from this process. It is also clear this algorithm produces a unique result in either direction. Thus, we have a bijection. □

3.5 Sundaram Tableaux and Ice Models

We follow the initial ice model conditions as described in Section 4. Additionally, we have the following boundary conditions:

1. The rightmost arrow of the first row always points out.
2. Further, the rows labeled with i and $\bar{i}$ are connected by a loop on the right hand side. They are either connected by an A or B loop.

3.5.1 Example

Let $\lambda = (3, 2, 0)$, and consider the following Gefland-Tsetlin-Type pattern:

$$\begin{array}{ccccc} 3 & & 2 & & 0 \\ & 3 & & 1 & \\ & & 2 & & 1 \\ & & & 2 & \\ & & & & 1 \end{array}$$

Then, Figure 3 shows an ice model with boundary arrows. Figure 4 shows the ice model with the boundary conditions and the Gelfand-Tsetlin-Type entries filled in. Finally, Figure 5 shows the fully filled-in ice model.

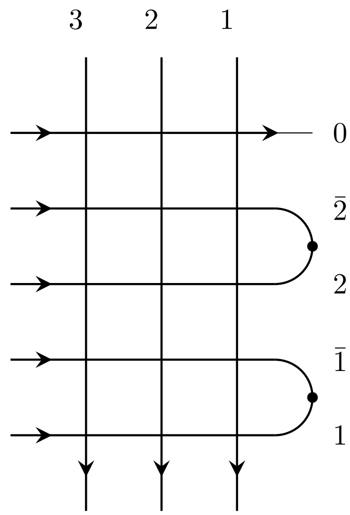

Figure 3

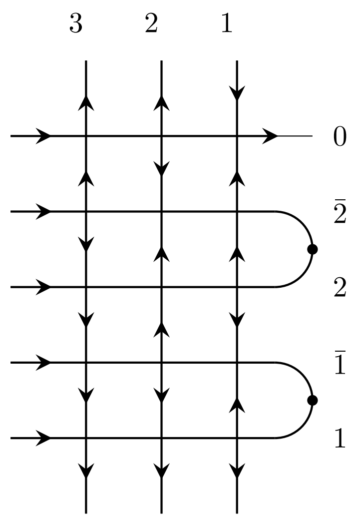

Figure 4

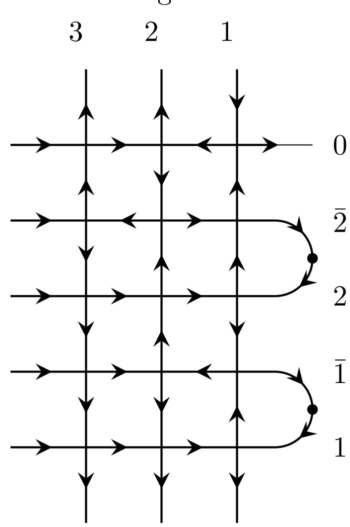

Figure 5

Lemma 3.5.1. *If $a_{2k+1,n-k+1} = 0$, then the loop on the right boundary indexed by $n-k+1$ and $\overline{n-k+1}$ goes counterclockwise. If not, then the loop goes clockwise. Further, in row 0, the arrow points out.*

Proof. We begin by proving the latter statement. Suppose instead of loops on the right side of our ice model, we create a new model where we include a column labeled 0. Let (x, y) denote the vertex of the ice model in column x and row y . First, because of our convention that the first row of the Gelfand-Tsetlin type pattern ends in 0, the the vertical arrow above the vertex $(0, 1)$ points up. Because of the second constraint on strict Gelfand-Tsetlin type patterns, the vertical arrow below vertex $(0, 1)$ points out. Thus, vertex $(0, 1)$ has two edges pointed out, and the other two arrows must point towards the vertex. Hence, in row 0, the far right arrow points out.

We now prove the first statement of the lemma. We make use of Lemma 2 in Section 4 from a paper by Brubaker, Bump, and Friedberg [1]. From this lemma, we get that, excluding the first row, the rightmost arrows (in the 0 column) must alternate in our model. Now we need to determine the edge above the $(2(n-k+1)+1, 0)$ vertex. Because of constraint 2 on strict Gelfand-Tsetlin type patterns, the edge below this vertex points away. By the edge to the right of the vertex points in. Thus, if $a_{2k+1,n-k+1} = 0$ in our GT pattern, then the arrow pointing above the $(2(n-k+1)+1, 0)$ vertex points up, and hence, the edge to the left of the $(2(n-k+1)+1, 0)$ vertex points towards it. Further, the edge to the left of the $(2(n-k+1), 0)$ vertex points away from the vertex. Hence, our loop will be counterclockwise. The argument uses the same reasoning if $a_{2k+1,n-k+1} \neq 0$. □

We use the following convention. We consider the state of a vertex to be either $\{NE, NS, NW, EW, SE, SW\}$, where the state is determined by which arrows pointed in towards the vertex. In particular, if the top edge points in and the right edge points in at a vertex, then we label it with NE.

Lemma 3.5.2. *No vertex in the top row has a state of NE if and only if the fourth condition of the Gelfand-Tsetlin Patterns is satisfied.*

Proof. First, suppose, toward a contradiction, that there exists a vertex with a NE state in the top row. In particular, this cannot be the top left vertex because the top left vertex always points from the West. Further, let us assume this is the left most NE vertex. Thus, the next vertex over must have top edge pointing away from the vertex. Now, if this is an EW state, then we have a contradiction, since the arrow pointing up on the top edge corresponds to an element λ_k of our initial partition. Further, condition 4 on our GT patterns imply that either λ_k or $\lambda_k - 1$ must appear in our second row of the GT pattern. Thus, the vertex next to NE must be a SE vertex. Suppose the next vertex is a EW vertex. Again we have a contradiction, because we have $\lambda_k + 1$ and λ_k appearing in our initial partition. Thus, at least two of $\lambda_k + 1$, λ_k, and $\lambda_k - 1$ must appear in the second row, but this is not the case. Thus, we must have another SE vertex. Thus suppose we have j SE vertices to the left of the NE vertex, and because of the construction, eventually we must get a vertex with EW vertex as the left side of our model points in. In this case, we have j+1 consecutive arrows pointing out on the top edges. However, we only have j arrows pointing up from the vertices of the second row. Thus, there exists an element in our GT pattern such that $a_{1,k} - a_{2,k} \nleq 1$. Then this vertex must have an EW configuration and the vertex to its right must be EW.

For the other direction, suppose, toward a contradiction, that the fourth rule is violated. Let $\alpha_1, ..., \alpha_n$ denote the spots where the arrows point up in a row and $\beta_1, ..., \beta_m$ denote the spots where the arrows point up in the row below it. Then there exists some α_i and β_i such that $\alpha_i > \beta_i + 1$. So we have the situation where the EW and NE configurations are forced and we obtain the desired contradiction. □

4 Deformation Formula for the Sundaram Case

Consider the ice models created in the Nathan Gray paper. Use the weights as he defines them. There is a bijection between his ice models and the alternating left boundary ice models found in Ivanov. Then, we have the following result:

Theorem 4.0.1. *Let $\lambda = (\lambda_n \geq \lambda_{n-1}, \geq \ldots, \geq \lambda_1 > 0)$ be a partition. Let $\rho = (n, n-1, \ldots, 2, 1)$. Let us create our ice models for $(\lambda + \rho)$ using our Gelfand-Tsetlin-type pattern rules from the Sundaram case. Using the Boltzmann weights as defined in Gray, let $\mathcal{Z}(\lambda)$ be the partition function defined on our ice states from the Sundaram case with top row $(\lambda + \rho)$. Let $C^* = \mathbf{z}^{-\rho} \prod_{i=1}^{n}(1 + tz_i^2) \prod_{i<j}(1 + tz_i z_j)(1 + z_i z_j^{-1})$, where $\mathbf{z}^{-\rho} = z_1^{-n} z_2^{-n+1} \ldots z_n^{-1}$. Let s_λ^{so} be the character of the irreducible representation of $SO(2n+1)$ indexed by λ. Then, $\mathcal{Z}(\lambda) = C^* s_\lambda^{so}$.*

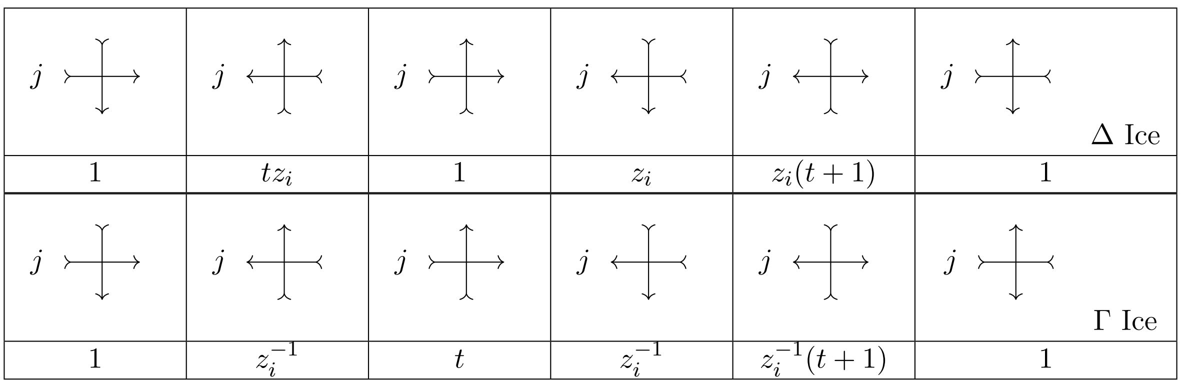

Figure 6: Boltzmann weights for Δ and Γ Sundaram Ice

Figure 7: Boltzmann Weights for Sundaram Bends

Proof. Using Ivanov and Gray, for top row $(\lambda + \rho)$ in the U-turn ice models, we have the partition function $\mathcal{Z}(\lambda) = C^* s_\lambda^{sp}$, where s_λ^{sp} is the character of the irreducible representation of $Sp(2n)$ indexed by λ. Now, in our ice models, every top row has a product equal to 1. Thus, eliminating this top row, we have an ice model exactly like those in Gray, where the top row is exactly the second row of our GT pattern. Thus, let $(\lambda' + \rho)$ be the second row of our GT pattern. Note that $|(\lambda + \rho)| = |(\lambda' + \rho)|$ by construction of our ice models. Also note that if $\lambda_1 > \lambda_1'$, the difference is exactly 1. Also, this implies every vertex in the first column of our ice models with top row $(\lambda' + \rho)$ is NW, which is a weight of 1. Thus, for any given top row $(\lambda' + \rho)$, we get $\mathcal{Z}(\lambda') = C^* s^{sp}_{\lambda'}$. Thus, if we consider all possible allowed second rows of our GT patterns, we get the following:

$$\mathcal{Z}(\lambda) = \sum_{\mu \subseteq \lambda} C^* s^{sp}_{\mu} \tag{20}$$

where $\mu \subseteq \lambda$ if it is an allowed second row in our GT model. However, as a result of Sundaram,

$$\sum_{\mu \subseteq \lambda} s^{sp}_{\mu} = s^{so}_{\lambda} \tag{21}$$

Thus, in particular, we get $\mathcal{Z}(\lambda) = C^* s^{so}_{\lambda}$ □

Now we are interested in a type B character deformation times a type B character. Through an adjustment of weights from Gray, we get the following.

Corollary 4.0.1. *There exists a set of Boltzmann weights for ice models in the Sundaram case such that the partition function defined from our ice models is precisely:*

$$\mathcal{Z}(\lambda) = \prod_{i=1}^{n}(1 + tz_i) \prod_{i<j}(1 + tz_i z_j)(1 + z_i z_j^{-1}) s^{so}_{\lambda} \tag{22}$$

Proof. Consider Theorem 1. Using the weights from Gray, we make the following modification: let A_i and B_i be the clockwise and counterclockwise oriented U-turn boundary connecting row i and $\bar{i}$, respectively. We note that either A_i or B_i occurs in every ice state. Thus, let us multiply our weights for A_i and B_i by $z_i^{-n+i-1}\dfrac{(1 + tz_i)}{(1 + tz_i^2)}$. Thus, this means for a given ice state, we are multiplying the weight of the model by $\mathbf{z}^{-\rho}\dfrac{\prod_{i=1}^{n}(1 + tz_i)}{\prod_{i=1}^{n}(1 + tz_i^2)}$. Since this happens for all our ice states, we are simply multiplying our partition function that we got from Theorem 1, by $\mathbf{z}^{-\rho}\dfrac{\prod_{i=1}^{n}(1 + tz_i)}{\prod_{i=1}^{n}(1 + tz_i^2)}$, giving the result. □

5 Koike-Terada Tableaux

5.1 Construction

Another set of tableaux rules for the $SO(2n + 1)$ group is defined by Koike and Terada in [9].
Given a partition $\lambda = (\lambda_n \geq \lambda_{n-1} \geq \cdots \geq \lambda_1 \geq 0)$, we fill a standard Young tableau of shape λ with the alphabet $\{1 < \bar{1} < \bar{\bar{1}} < 2 < \bar{2} < \bar{\bar{2}} \cdots n < \bar{n} < \bar{\bar{n}}\}$. Let $T_{i,j}$ be the entry of the tableau in the i-th row and the j-th column. The filling of the tableau must satisfy the following conditions:

1. k can only appear in $T_{k,1}$
2. Rows are weakly increasing
3. Columns are strictly increasing
4. $T_{i,j} \geq i$

Given a tableau filled according to these rules, the weight of the tableau is consequently defined.

Definition 5.1.1. Let T be a tableau of shape λ. The **weight** of T is the vector of integers $wt(T) = (d_1, d_2, \ldots, d_n)$, where $d_i = w(\bar{i}) - w(\bar{\bar{i}})$ denotes the difference between the number of $\bar{i}$'s and $\bar{\bar{i}}$'s in T.

We let $\mathbf{z}^{wt(T)} = z_1^{d_1} z_2^{d_2} \cdots z_n^{d_n}$. Then, summing over all tableaux of shape λ yields the character formula.

5.2 Young-Diagrammatic Description of Branching Rules

Koike and Terada gave a description of the restriction rules of representations of $SO(2n+1,\mathbb{C})$ using these tableaux. Instead of using the Gelfand-Tsetlin bases of representation spaces as in Zhelobenko [16], the tableaux rules given above directly determine the weights and multiplicities in an irreducible representation of the special orthogonal group.
Let λ be a partition. The length of λ is the number of non-zero terms and is denoted by $l(\lambda)$. A subpartition $\lambda \supset \mu = (\mu_n, \mu_{n-1}, \ldots, \mu_n - m + 1)$ is a partition of length $m \leq n$ such that $\mu_i \leq \lambda_i$, for all $n - m \leq i \leq n$. In other words, the Young diagram of λ contains the diagram of μ. The skew diagram is the set-theoretic difference $\theta = \lambda - \mu$. [11]
Under the restriction rule $SO(2n+1) \downarrow SO(2n-1) \times GL(1)$, the character of the irreducible representation parametrized by λ is related to the tableaux as follows:

$$\chi_{\lambda_{SO(2n+1)}} \downarrow SO(2n-2k+1) \times \overbrace{GL(1) \times \cdots \times GL(1)}^{k \text{ times}} = \sum_{\substack{\mu \subset \lambda, l(\mu) \leq n-k \\ T_{\lambda-\mu}}} \chi_{\mu_{SO(2n-2k+1)}} \cdot z^{wt(T)}, \quad (23)$$

where the summation runs over all possible fillings of skew tableaux of $\lambda - \mu$.
In lieu of proving Equation 23, which can be done inductively, we look at the case of $k = 1$, i.e. branching down one level. Each skew tableau gives rise to a monomial in z_n, hence the character of a representation of $GL(1)$. The tableaux of shape λ thus illustrate how a polynomial representation of $SO(2n+1)$ decomposes as a direct sum of irreducible representations of its subgroups upon restriction to $SO(2n-1) \times GL(1)$. Although this description of restriction rules is independent of Gelfand-Tsetlin bases, we develop an analogue of such patterns in the next section.

5.3 Gelfand-Tsetlin-Type Patterns

We developed Gelfand-Tsetlin-type patterns in bijection with the Koike-Terada tableaux. Let $a_{i,j}$ be the entry of the pattern in the i-th row and the j-th column. Given a partition $\lambda = (\lambda_n \geq \lambda_{n-1} \geq \cdots \geq \lambda_1 \geq 0)$, we create a pattern with top row λ satisfying the following rules:

1. The pattern has $3n$ rows. We will label these rows $1, \bar{1}, \bar{\bar{1}}, \cdots, n, \bar{n}, \bar{\bar{n}}$, starting from the bottom of the pattern.

2. Rows $i, \bar{i}$, and $\bar{\bar{i}}$ must have i entries that weakly decrease across the row.

3. Each entry b must be in the interval $[a, c]$, where a is the entry above and to the right of b, and c is the entry above and to the left of b.

4. Row i must end in a 1 or a 0 (for $i \in \{1, \cdots, n\}$)

5. Each entry in row $\bar{\bar{i}}$ (for $\bar{\bar{i}} \in \{\bar{\bar{1}}, \cdots, \overline{\overline{n-1}}\}$) must be left-leaning.

Rules 4 and 5 account for the first tableaux rule.
The correspondence between the Koike-Terada tableuax and Gelfand-Tsetlin-type patterns works in the same way as in the Sundaram case.

Example 5.3.1. The Gelfand Tsetlin-type pattern

$$\begin{array}{cccccc} 5 & & 3 & & & \\ & 4 & & 2 & & \\ & & 2 & & 1 & \\ & & & 2 & & \\ & & & & 1 & \\ & & & & & 0 \end{array} \tag{24}$$

corresponds with the tableau

$\bar{1}$	$\bar{\bar{1}}$	$\bar{2}$	$\bar{2}$	$\bar{\bar{2}}$
2	$\bar{2}$	$\bar{\bar{2}}$		

5.4 Shifted Tableaux and Strict Gelfand-Tsetlin-type patterns

Just like in the previous section, we want to to define a bijection between shifted tableaux and strict Gelfand-Tsetlin-type patterns to construct corresponding ice models. We refer to a Gelfand-Tsetlin-type pattern as strict if each row is strictly increasing from right to left. Then the shifted tableaux rules are defined as follows:

1. Rows are weakly increasing.

2. Columns are weakly increasing.

3. Diagonals are strictly increasing.

4. The first entry in row k is k, $\bar{k}$ or $\bar{\bar{k}}$.

We note that violation of the fifth rule would result in the following configuration in the Gelfand-Tsetlin-type pattern (thus contradicting its strictness):

$$\begin{array}{ccccccc} c & & 0 & & 0 & & \\ & c & & 0 & & & \\ & & c & & 0 & & \\ & & & c & & 0 & \\ & & & & c & & \\ & & & & & b & \\ & & & & & & a \end{array} \tag{25}$$

5.5 Ice Model

The next step in the characterization of Koike-Terada tableaux is to construct an ice model in bijection with strict patterns.

We define our ice model to be a grid with $3n$ horizontal and λ_n vertical lines. The horizontal lines are labeled from 1 to $\overline{\overline{n}}$ starting from the bottom and the vertical lines are labeled 1 to λ_n starting from the right. The shape and boundary conditions are given as follows:

We allow the three possible "bends" on the right boundary of each model connecting the rows labeled $\overline{\overline{k}}$ and $\overline{k}$ for each $k \in \{1, \cdots, n\}$:

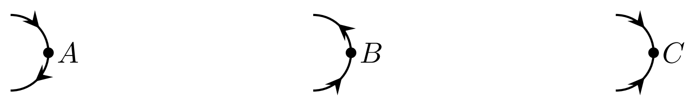

Note that the loop of the type  is not possible, as it would require having two consecutive NS configurations in the same column, which clearly can't happen. We also allow the three possible configurations called "ties" on the right boundary of each row labeled $k \in \{1, \cdots, n\}$:

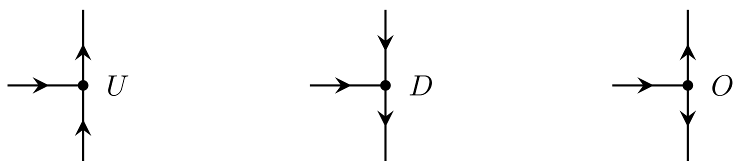

Furthermore, every row labeled $k \in \{1, \cdots, n\}$ is a three-vertex model: the only vertex configurations are SW, NW, and NE.

The next three figures demonstrate boundary conditions and the full ice model for one of the patterns of $\lambda = (2, 1)$.

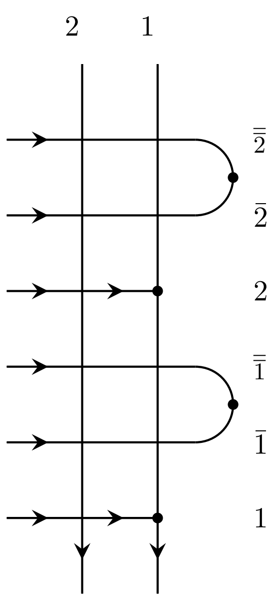

Figure 8: Boundary

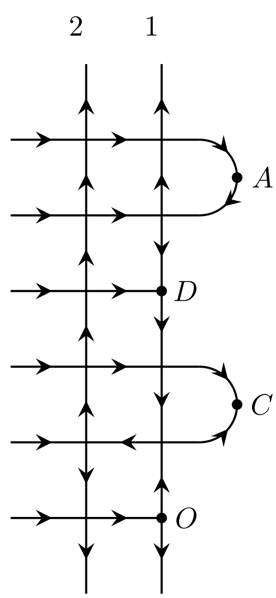

Figure 9: Ice Model

2		1				
	2		1			
		2		0		
			2			
				2		
					1	

Figure 10: GT pattern

We prove that such ice models are in bijection with strict Gelfand-Tsetlin-like patterns in the next two theorems. We note that the first three Gelfand-Tsetlin-type pattern rules are automatically satisfied as in previous sections. It remains to prove the bijection between the strict Gelfand-Tsetlin-type patterns and the ice, which we will do with the following theorem:

Theorem 5.5.1. *The following are equivalent:*

1. *Koike-Terada Gelfand-Tsetlin-type pattern rules 4 and 5 are satisfied.*
2. *Each ice row labeled $k \in \{1, \cdots, n\}$ has no NS, SE, or EW configurations, and tie boundary conditions are satsified.*

Proof. We'll show the two directions: First, suppose that rules 4 and 5 are satisfied. Then clearly NS isn't possible in rows labeled k, since all the entries in row $\overline{\overline{k-1}}$ are left-leaning. Now assume, toward a contradiction, that we have a SE configuration in a row labeled k. Then the configuration to the left of it is either SE again, or NE, or EW. If it is SE or NE, we look at the configuration to the left of it. We may now assume we reached the leftmost SE or NE configuration, then the state to the left must be EW because of the left boundary conditions. But this is a contradiction to rule 5, since we get a non-left-leaning entry, as the up-arrow in the EW configuration is not the rightmost in that row.

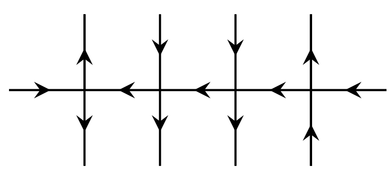

Figure 11: SE forces EW

Now we note that rule 4 directly implies that we cannot have EW in any row labeled $k \in \{1, ..., n\}$. A Gelfand-Tsetlin-type pattern row ending in 0 or 1 implies that we could only have EWin the (imaginary) 0^{th} or 1^{st} row, and none of these are possible.

We will now show that the tie boundary conditions are also implied by rules 4 and 5. So, row k must end in a 0 or a 1. If row k ends in a 1, then a 1 cannot appear in row $\overline{\overline{k-1}}$ since each entry in row $\overline{\overline{k-1}}$ must be left-leaning and strictly decreasing. This would correspond to having an EW in column 1 of our ice model if we had a full column 1, but now corresponds to the O-tie. If row k ends in a 0, then for similar reasoning we would have an EW in the 0^{th} column of our ice model, if we were to have a 0^{th} column. As stated earlier, we know SE and NS cannot appear in this row, and it is clear that neither EW nor NE can appear directy to the left of an EW. Thus, the only possible fillings for the vertex in the 1^{st} column would be a SW or a NW. Having a SW implies having the U tie boundary, and having a NW implies the type D tie boundary.

First, suppose each non-bar row has no NS, SE, and EW. Then, the only vertices in the row can be NW, SW, and NE. Each of these types of vertices have the two vertical arrows pointing in the same direction, meaning the row below it is left leaning. Thus, rule 5 is satisfied. Next, suppose the tie boundary conditions are also satisfied. Then assume, toward a contradiction, that row $k \in \{1, \cdots, n\}$ ends in a number greater than 1. This means the only possible tie configuration for row k would be D. If this is the case, all the horizontal arrows to the left of it must point right to avoid NS. However, since row k in the Gelfand-Tsetlin-type pattern has one more entry than row $\overline{\overline{k-1}}$, then eventually we will have a configuration where two consecutive vertical arrows in that row point away from each other, thus obtaining the desired contradiction, and rule 4 is satisfied. □

6 Proctor Tableaux

6.1 Construction

We will examine one more tableaux associated to $SO(2n+1)$, as defined by Proctor.Let $\lambda = (\lambda_n \geq \lambda_{n-1} \geq \cdots \geq \lambda_1 \geq 1)$ be a partition. We fill a standard Young Tableaux of shape λ with alphabet and ordering $\{1 < 2 < \cdots < 2n < 0\}$, where 0 is infinity. We define $T_{i,j}$ to be the entry in a tableaux T in row i and column j. We fill the tableaux such that:

1. Rows are weakly increasing.
2. Columns are strictly increasing.
3. Follows the $2c$ orthogonal condition
4. Follows the $2m$ protection condition

Definition 6.1.1. The $2c$ **orthogonal condition** is satisfied if for every $c \leq n$, there are less than or equal to $2c$ entries that are less than or equal to $2c$ in the first two columns, not including a 0 entry.

Definition 6.1.2. The $2m$ **protection condition** is satisfied if for every $m \leq n$:

1. If an entry in the first column is equal to $2m-1$, then define i to be equal to the row number of said entry.
2. Then, define k to be equal to $2m - i$.
3. If there is an entry in the kth row equal to $2m$, let h be equal to the column number of the leftmost $2m$ entry.
4. Then, for any j such that $2 \leq j \leq h$, $T_{k,j}$ must be equal to $2m-1$. Additionally, $T_{k-1,h}$ must equal to 2m-1.
5. If the suppositions do not hold for m, then the condition is trivially satisfied.

For example, if our tableaux looked like the following:

$$\begin{array}{|c|c|c|c|} \hline 1 & 1 & x & 5 \\ \hline 3 & x & 4 \\ \cline{1-3} 5 \\ \cline{1-1} \end{array} \tag{26}$$

Then to satisfy the $2m$ protection condition, every entry where there is an x (i.e. $T_{1,3}$ and $T_{2,2}$) must equal 3. If our tableaux looked like the following:

$$\begin{array}{|c|c|c|c|}\hline 1 & 1 & 3 & 5 \\ \hline x & 3 & 4 \\ \cline{1-3} 5 \\ \cline{1-1}\end{array} \tag{27}$$

Then the entry $T_{2,1}$ must be greater than or equal to 3 in order to satisfy the 2c orthogonal rule (and, in this case, it must be 3 so that the 2nd row is weakly increasing). If $T_{2,1}$ were equal to 2, then when $c = 1$, there would be more than $2c$ entries in the first two columns that are less than or equal to $2c$. The following tableaux satisfies all of the rules of a valid Proctor tableaux:

$$\begin{array}{|c|c|c|c|}\hline 1 & 1 & 3 & 5 \\ \hline 3 & 3 & 4 \\ \cline{1-3} 5 \\ \cline{1-1}\end{array} \tag{28}$$

6.2 Branching Rules

We have that the indexing set for these two point-wise equal sets of positive tensor orthogonal characters coincide for all n for $SO(2n + 1)$ and O_{2n+1}. The rules for Proctor's tableaux are a consequence of the branching restriction $O_{2n+1} \downarrow O_{2n-1} \otimes O_2$ at each step, where the restriction to O_{2n-1} gives us the Protection Condition and the restriction to O_2 gives us the Orthogonal Condition. Proctor gives the following proposition.

Proposition 6.2.1. Proctor 10.3 Let $G_N = O_N$, and let λ respectively be an N-orthogonal partition. Then the representation $G_N(\lambda)$ restricts to $\oplus G_{N-2}(v) \otimes G_2(\lambda - v)$, where the sum is over all $v \subseteq \lambda$ which are possible indexing partitions for representations of G_{N-2} such that $\lambda - v$ does not have more than 2 boxes in a column.

6.3 Proctor Tableaux and Gelfand-Tsetlin-Type Patterns

To create Gelfand-Tsetlin-type patterns to correspond with the odd special orthogonal tableaux rules given by Proctor, we must take into consideration the effect of the $2c$ orthogonal condition and the $2m$ protection condition. We begin with our top row entries being equal to λ. The top n rows will have n entries. The n+1st row will have $n - 1$ entries, the $n + 2$nd row will have $n - 2$ entries, etc, and the bottom row will have 1 entry.

To biject with the 2m protection condition, we use the following rules in our patterns.

- In order to check the following rules, all of the rows in our Gelfand-Tsetlin-type patterns must have n entries. We add 0s to the ends of our rows that have less than n entries such that each row now has n entries (including the added 0's). Additionally, we add a "0th row" at the bottom of our Gelfand-Tsetlin-type pattern that is made of n 0's.
- If there is a non-left-leaning 0 entry in an even row, we define m and i so that $a_{2m-2,i} = 0$.
- Then, define $j = 2m - i$.
- We check to see if $a_{2m,j} \geq a_{2m-1,j}$. If it is, we check the following:

- $a_{2m-1,j-1} \geq a_{2m-2,j-1}$.
- $a_{2m-1,j-1} \geq a_{2m,j}$
- $a_{2m-2,j} \leq 1$

To biject with the $2c$ orthogonal condition, we have a restriction on the entries in an even row, $2c$. For entries in the $2c$ row, let the orthogonal sum be the sum of the entries such that for $1 \leq k \leq n$, $a_{2c,k} = a_{2c,k}$ for $a_{2c,k} \leq 2$ and $a_{2c,k} = 2$ for $a_{2c,k} > 2$. This sum must be less than or equal to $2c$.

6.4 Proctor Tableaux and Ice

Using the above restrictions on Gelfand-Tsetlin-type patterns, we show that corresponding ice models do not follow naturally. In the Sundaram and Koike-Terada bijections to ice, only Gelfand-Tsetlin-type patterns that are strictly decreasing across rows have corresponding ice models. Non-strict Gelfand-Tsetlin-type patterns do not have corresponding statistical mechanical meaning in the form of ice models.

Proposition 6.4.1. There exists no ice model in bijection with Proctor tableaux.

Proof. In the case of $n = 4$, we can look at the fourth row. The smallest possible strict configuration would be $\lambda_4 = 3, 2, 1, 0$. However, the orthogonal sum of that row, according to the orthogonal restrictions on Gelfand-Tsetlin-type patterns, is 5, which is greater than 4, thus breaking the restriction. Therefore, in the case of $n = 4$, there are no strict Gelfand-Tsetlin-type patterns, and consequently no valid ice models. □

7 Concluding Remarks

Now that we have a deformation formula and corresponding ice models for Cartan type B, the question is: how "good" are our weights? It turns out that the ice models appear in special analytic L-functions. In particular, when considering the Fourier expansion, the weights of the ice models are precisely the coefficients in the expansion. Thus, the next step would be to turn towards analytic number theory to see the usefulness of our results. We also still have other ice models that could be assigned weights. Koike-Terada tableaux rules produce valid statistical mechanical ice models. Thus, determining weights for these ice models and producing a type B Weyl character deformation would be useful. We note that there does not seem to be any research on ice models for Cartan type D. Thus, a potential future research direction is considering the type D case.

8 Acknowledgements

This research was conducted at the 2018 University of Minnesota-Twin Cities REU in Algebraic Combinatorics. Our research was supported by NSF RTG grant DMS-1745638. We thank Benjamin Brubaker and Katherine Weber for their advice and support during our time in the Twin Cities. We also thank Jiyang Gao for his contributions to the project.

References

[1] Ben Brubaker, Daniel Bump, and Solomon Friedberg. "Schur Polynomials and The Yang-Baxter Equation". en. In: *Communications in Mathematical Physics* 308.2 (Dec. 2011), pp. 281–301.

[2] Ben Brubaker and Andrew Schultz. "The six-vertex model and deformations of the Weyl character formula". en. In: *Journal of Algebraic Combinatorics* 42.4 (Dec. 2015), pp. 917–958.

[3] Markus Fulmek and Christian Krattenthaler. "A bijection between Proctor's and Sundaram's odd orthogonal tableaux". In: *Discrete Mathematics* 161.1 (1996), pp. 101 –120.

[4] Nathan Gray. "Metaplectic Ice for Cartan Type C". PhD thesis. Sept. 2017.

[5] A.M. Hamel and R.C. King. "Symplectic Shifted Tableaux and Deformations of Weyl's Denominator Formula for sp(2n)". In: *Journal of Algebraic Combinatorics* 16.3 (Nov. 2002), pp. 269–300.

[6] Roger Howe et al. "A reciprocity law and the skew Pieri rule for the symplectic group". In: *Journal of Mathematical Physics* 58 (Nov. 2016).

[7] Dmitriy Ivanov. "Part I, Symplectic ice, Part II, Global and local Kubota symbols". PhD thesis. Aug. 2010.

[8] R.C. King and N.G.I. El-Sharkaway. "Standard Young tableaux and weight multiplicities of the classical Lie groups". In: *Journal of Physics A: Mathematical and General* 16.14 (1983), p. 3153.

[9] Kazuhiko Koike and Itaru Terada. "Young diagrammatic methods for the restriction of representations of complex classical Lie groups to reductive subgroups of maximal rank". en. In: *Advances in Mathematics* 79.1 (Jan. 1990), pp. 104–135.

[10] Greg Kuperberg. "Symmetry Classes of Alternating-Sign Matrices under One Roof". In: *The Annals of Mathematics* 156.3 (Nov. 2002), p. 835.

[11] I. G. Macdonald. *Symmetric functions and Hall polynomials*. Reprinted in paperback. Oxford classic texts in the physical sciences. Oxford: Clarendon Press, 2015.

[12] Soichi Okada. "Alternating Sign Matrices and Some Deformations of Weyl's Denominator Formulas". In: *Journal of Algebraic Combinatorics* 2.2 (1993), pp. 155–176.

[13] R.A. Proctor. "Young Tableaux, Gelfand Patterns, and Branching Rules for Classical Groups". en. In: *Journal of Algebra* 164.2 (Mar. 1994), pp. 299–360.

[14] Sheila Sundaram. "Orthogonal tableaux and an insertion algorithm for SO(2n + 1)". In: *Journal of Combinatorial Theory, Series A* 53.2 (Mar. 1990), pp. 239–256.

[15] Takeshi Tokuyama. "A generating function of strict Gelfand patterns and some formulas on characters of general linear groups". en. In: *Journal of the Mathematical Society of Japan* 40.4 (Oct. 1988), pp. 671–685.

[16] D P Zhelobenko. "The Classical Groups. Spectral Analysis of Their Finite-Dimensional Representations". In: *Russian Mathematical Surveys* 17.1 (Feb. 1962), pp. 1–94.

Yulia Alexander, Department of Mathematics and Computer Science, Wesleyan University, Middletown, CT 06459
E-mail address: yalexandr@wesleyan.edu

Patricia Commins, Department of Mathematics and Statistics, Carleton College, Northfield, MN 55057
E-mail address: comminsp@carleton.edu

Alexandra Embry, Department of Mathematics, Indiana University, Bloomington, IN 47405
E-mail address: aiembry@iu.edu

Sylvia Frank, Department of Mathematics and Statistics, Amherst College, Amherst, MA 01002
E-mail address: sfrank20@amherst.edu

Yutong Li, Department of Mathematics and Statistics, Haverford College, Haverford, PA 19041
E-mail address: yli11@haverford.edu

Alexander Vetter, Department of Mathematics and Statistics, Villanova University, Villanova, PA 19085
E-mail address: avetter@villanova.edu